Molecular Neurobiology (2020) 57:1115–1130
https://doi.org/10.1007/s12035-019-01795-3

White Matter Abnormalities Linked to Interferon, Stress Response, and Energy Metabolism Gene Expression Changes in Older HIV-Positive Patients on Antiretroviral Therapy

Isaac H. Solomon[1,2] · Sukrutha Chettimada[2] · Vikas Misra[2] · David R. Lorenz[2] · Robert J. Gorelick[3] · Benjamin B. Gelman[4] · Susan Morgello[5] · Dana Gabuzda[2,6]

Received: 9 July 2019 / Accepted: 22 September 2019 / Published online: 5 November 2019

Abstract

Neurocognitive impairment (NCI) remains a significant cause of morbidity in human immunodeficiency virus (HIV)-positive individuals despite highly active antiretroviral therapy (HAART). White matter abnormalities have emerged as a key component of age-related neurodegeneration, and accumulating evidence suggests they play a role in HIV-associated neurocognitive disorders. Viral persistence in the brain induces chronic inflammation associated with lymphocytic infiltration, microglial proliferation, myelin loss, and cerebrovascular lesions. In this study, gene expression profiling was performed on frontal white matter from 34 older HIV+ individuals on HAART (18 with NCI) and 24 HIV-negative controls. We used the NanoString nCounter platform to evaluate 933 probes targeting inflammation, interferon and stress responses, energy metabolism, and central nervous system-related genes. Viral loads were measured using single-copy assays. Compared to HIV− controls, HIV+ individuals exhibited increased expression of genes related to interferon, MHC-1, and stress responses, myeloid cells, and T cells and decreased expression of genes associated with oligodendrocytes and energy metabolism in white matter. These findings correlated with increased white matter inflammation and myelin pallor, suggesting interferon (IRFs, IFITM1, ISG15, MX1, OAS3) and stress response (ATF4, XBP1, CHOP, CASP1, WARS) gene expression changes are associated with decreased energy metabolism (SREBF1, SREBF2, PARK2, TXNIP) and oligodendrocyte myelin production (MAG, MOG), leading to white matter dysfunction. Machine learning identified a 15-gene signature predictive of HIV status that was validated in an independent cohort. No specific gene expression patterns were associated with NCI. These findings suggest therapies that decrease chronic inflammation while protecting mitochondrial function may help to preserve white matter integrity in older HIV+ individuals.

Keywords HIV-associated neurocognitive disorders · White matter · Inflammation · Interferon response · Stress response · Oxidative stress · Aging

Isaac H. Solomon and Sukrutha Chettimada contributed equally to this work.

Electronic supplementary material The online version of this article (https://doi.org/10.1007/s12035-019-01795-3) contains supplementary material, which is available to authorized users.

✉ Dana Gabuzda
dana_gabuzda@dfci.harvard.edu

[1] Department of Pathology, Brigham and Women's Hospital, Boston, MA, USA

[2] Department of Cancer Immunology and Virology, Dana-Farber Cancer Institute, CLS 1010, 450 Brookline Ave, Boston, MA 02215, USA

[3] AIDS and Cancer Virus Program, Frederick National Laboratory for Cancer Research, Frederick, MD, USA

[4] Department of Pathology, University of Texas Medical Branch, Galveston, TX, USA

[5] Department of Neurology, Icahn School of Medicine of Mount Sinai, New York, NY, USA

[6] Department of Neurology, Harvard Medical School, Boston, MA, USA

Introduction

Despite the availability of highly active antiretroviral therapy (HAART) leading to undetectable viral loads, neurocognitive impairment (NCI) remains a significant cause of morbidity for individuals infected with human immunodeficiency virus (HIV) [1, 2]. Mechanisms underlying the pathogenesis of HIV-associated neurocognitive disorders (HAND), which include asymptomatic neurocognitive impairment (ANI), minor neurocognitive disorder (MND), and HIV-associated dementia (HAD), remain incompletely understood [3]. HIV has been reported to accelerate aging, characterized by earlier onset of symptoms due to mechanisms such as immunological senescence and metabolic abnormalities, and to accentuate aging in virally suppressed individuals on HAART by acting as an additional risk factor for increased NCI across all ages [4]. HIV DNA remains detectable in the brain, particularly in white matter, in most HIV+ individuals despite plasma viral suppression on HAART, indicating a persistent reservoir for HIV reactivation from latency [5, 6]. Chronic inflammation, impaired proteostasis, and cerebrovascular disease are associated with chronic HIV infection and aging, and may lead to neurodegeneration and NCI [7–9]. Microglial activation and T cell infiltration are increased in the white matter of HIV+ individuals with and without HIV-encephalitis (HIVE), normal aging, and neurodegenerative diseases including Alzheimer's disease [10–12]. Gene expression studies have identified marked changes in the brains of untreated individuals with HIVE, including upregulation of genes related to interferon responses, antigen presentation, and complement components; these changes are similar but milder in HAART-treated individuals [13, 14]. Additional factors contributing to HAND pathogenesis are likely to include effects of some antiretroviral drugs and comorbidities common in the HIV+ population, including drug and alcohol use and co-infections (e.g., hepatitis C virus) [15–17].

White matter dysfunction has emerged as a key component of age-related neurodegeneration and HIV-associated neurocognitive impairment, likely due to the role of white matter axons in brain connectivity. Premortem neuroimaging studies have identified white matter abnormalities in HIV-infected individuals on HAART as well as older uninfected individuals, including increased white matter hyperintensities and other white matter lesions, decreased white matter integrity, and increased gap between predicted and chronological brain age [16, 18–22]. Histological correlates of white matter lesions include myelin pallor, tissue rarefaction, oligodendrocyte loss, diffuse axonal injury, and reactive gliosis, as well as vascular abnormalities including small-vessel arteriolosclerosis, microinfarcts, and hemorrhages [19]. These nonspecific findings are also frequent in HIV+ patients without HIVE, suggesting overlapping mechanisms [11, 23, 24]. Decreased oligodendrocytes and myelin density are associated with aging and vascular dementia, due in part to the susceptibility of myelin-associated glycoprotein (MAG) to ischemia, and accumulation of degenerating myelin basic protein (MBP) [19]. Ischemic injury is associated with increased production of reactive oxygen species and oxidative stress, which can be counteracted by various protective mechanisms including activity of the detoxifying enzyme heme oxygenase-1 (HO-1) and regulation of mitochondrial biogenesis by transcriptional factor A (TFAM) [25, 26]. In astrocytes, HIV-associated inflammation and oxidative stress are associated with elevated calcium levels, activation of the unfolded protein response, and mitochondrial dysfunction [27]. To better understand pathways underlying HAND pathogenesis, we assembled a cohort of 58 subjects (34 HIV+ and 24 HIV−) with available postmortem frozen brain tissue and evaluated gene expression patterns (n = 933 genes) in frontal lobe subcortical white matter using the NanoString nCounter platform.

Methods

Cohort Selection and Characterization

A cohort of older HIV+ patients (defined as ≥ age 45 at death) and age-matched HIV-negative controls with available frozen autopsy brain tissue collected between 2000 and 2014 was assembled from the National NeuroAIDS Tissue Consortium (NNTC) sites (Texas NeuroAIDS Research Center, National Neurological AIDS Bank, Manhattan HIV Brain Bank, and California NeuroAIDS Tissue Network). All subjects were enrolled with written informed consent and institutional review board (IRB) approval at each study site. Autopsy tissue samples and demographic, clinical, and laboratory data were collected and coded to protect participants' confidentiality in accordance with IRB-approved protocols at the University of Texas Medical Branch, University of California Los Angeles, Icahn School of Medicine at Mount Sinai, University of California San Diego, and Dana-Farber Cancer Institute. To identify older HIV− controls, we searched the NNTC database for persons aged 45–80 years with no history of HIV. To identify older HIV+ cases, we searched for participants aged 45–80 years on HAART for at least 1 year, including the year prior to death, with a recorded last premortem plasma viral load (VL) within 12 months prior to death of < 1000 HIV RNA copies/mL or undetectable (< 50 or 400 copies/mL, depending on the year that testing was performed). Cases with fatal stroke, CNS hemorrhage, multiple sclerosis, and active CNS infections were excluded. The following cases not meeting all search or exclusion criteria were included: three cases under age 45 (range 40–43) and two HIV+ cases with last plasma VL > 1000 copies/mL (range, 4953–8429). NCI status was determined based on HAND diagnoses and neurocognitive T scores. Five subjects with diagnoses reported

as neuropsychological impairment due to other causes (NPI-O) were assigned to the unimpaired group because review of available clinical data suggested a low likelihood of HAND based on neurocognitive *T* scores near the normal range and/or confounding by alcohol use. Clinical characteristics of each HIV+ subject are listed in Table S1.

Neuropathologic Examination

Brains were removed and examined at the individual NNTC sites [28]. Representative tissue was frozen or formalin-fixed and paraffin-embedded per consortium protocols, and hematoxylin and eosin stains were examined by neuropathologists at each site, with additional stains performed as necessary for individual cases. Features evaluated include type and extent of inflammation, presence of reactive astrocytes including Alzheimer type 2 astrocytes, presence of microglia or microglial nodules, evidence of cerebrovascular abnormalities including arterio- and arteriolosclerosis, age and size of ischemic lesions, abnormalities in myelination, presence of primary or secondary neoplasia, involvement by opportunistic infections, and evidence of non-HAND neurodegenerative disease. Cerebrovascular scores were defined as 0 = none, 1 = hypoxic-ischemic changes limited to cerebellar and/or hippocampal neurons, and 2 = arteriosclerosis, atherosclerosis, and/or ischemic infarcts. HIVE scores were defined as 0 = no or minimal inflammation, 1 = mild to moderate lymphocytic inflammation, and 2 = microglial nodules, severe lymphocytic inflammation, and/or leukoencephalopathy.

Nucleic Acid Extraction and Brain HIV Viral Load Measurements

Frontal lobe subcortical white matter RNA and DNA were simultaneously extracted from 10–15 mg frozen tissue using the AllPrep DNA/RNA isolation kit according to the manufacturer's instructions (Qiagen, Valencia, CA). Thirty-four paired samples of RNA and DNA from the HIV+ cases were assayed for HIV brain viral loads by the HIV Molecular Monitoring Core (HMMC) (Frederick National Laboratory for Cancer Research, Frederick, MD) using the HMMC gag assay [29], which measures an HIV-1 gag target. Input nucleic acid from 1–2 million cell equivalents (0.5–2 μg) was assayed in 12 replicates for each RNA and DNA sample. HIV-1 RNA values from two subjects were excluded from further analysis due to HIV-1 DNA contamination, evaluated by omission of reverse transcriptase. No inhibition was observed in any of the RNA or DNA samples, as assessed by spiking with HIV-1 gag transcript. DNA cell equivalent-recoveries were assessed using the hCCR5 assay [30] with each diploid cell containing two copies of the hCCR5 gene, which was used to normalize cellular HIV-1 RNA and DNA viral loads.

Gene Expression Profiling

The workflow for gene expression analysis is shown in Fig. 1. RNA content and quality (RNA integrity number, RIN) were evaluated using the Agilent BioAnalyzer (Agilent Technologies, Santa Clara, CA). mRNA hybridization, detection, and scanning were performed using NanoString nCounter technology and software (NanoString Technologies, Seattle, WA) [31] at the Dana-Farber/Harvard Cancer Center Molecular Biology core facility, as described [24]. The probeset consisted of 770 probes from nCounter PanCancer Immune Profiling Panel and 163 custom probes, targeting genes involved in stress responses (oxidative stress, ER stress, heat shock proteins, sirtuins), autophagy, energy metabolism, tryptophan metabolism, lipid metabolism, blood-brain barrier, neurodegeneration, and cell-type markers of neurons, astrocytes, oligodendrocytes, myeloid cells, and endothelial cells. The probes are listed in Table S2, and genes used as cell-type markers are listed in Table S3. Quality control checks were performed using nSolver 3.0 software (NanoString Technologies, Seattle, WA). Normalization

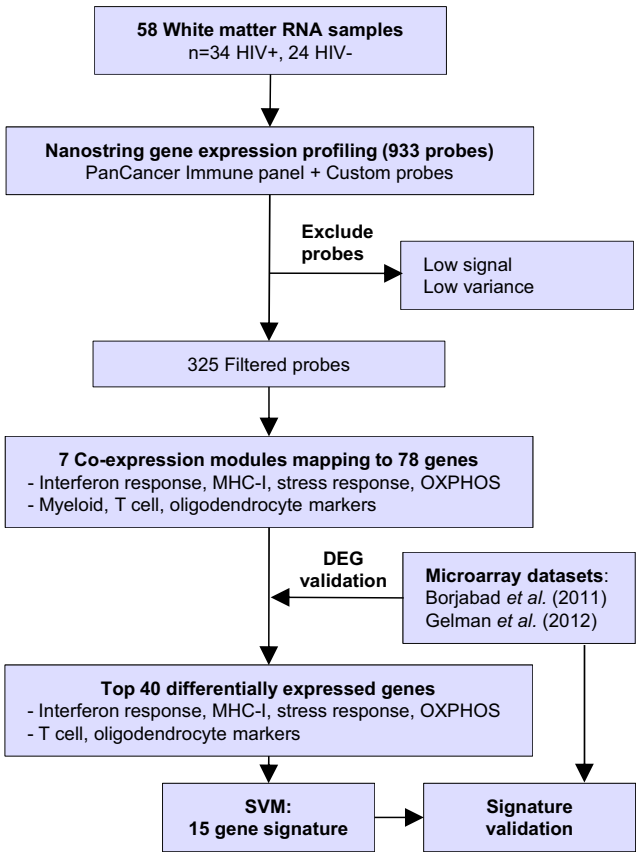

Fig. 1 Workflow for analysis of gene expression data. RNA was extracted from frozen frontal lobe subcortical white matter from 34 HIV+ and 24 age-matched HIV-negative subjects. Expression of 933 genes was analyzed to identify co-expression modules, differentially expressed genes, and SVM-based 15-gene signature. DEG, differentially expressed genes

between samples was performed using the cyclic loess method in the R *limma* package [32]. To adjust for background, mean signals from four negative control probes with the lowest mean counts were subtracted from all probe counts on a per-sample basis. Following initial analysis of RNA from 64 cases, 6 cases were excluded due to low RNA quality or high expression of neuronal markers (GRIN1, GRIN2A, GRIN2B, SNAP25, SYN1), leaving 58 cases for analysis of gene expression.

Data Analysis

Group differences in cohort characteristics, laboratory data, and neuropathological evaluation were determined by Student's *t* test or Fisher's exact test for continuous and categorical variables, respectively (P values < 0.05). For fold-change analysis of gene expression using NanoString technology, P values were calculated using Welch's *t* test ($P < 0.05$) and Pearson's correlation analyses were performed using R version 3.3.1. False-discovery rates (FDR) for gene expression profiling were estimated using the *fdrtool* package in R. Semi-supervised heatmaps, imputations for missing values based on k-nearest neighbors (KNN) [33], principal component analysis (PCA), k-means clustering, and support vector machine (SVM) analysis were performed using Qlucore Omics explorer software package version 3.3 (Qlucore AB, Lund, Sweden). Networks were generated using Ingenuity Pathways Analysis software (IPA; QIAGEN Inc., https://www.qiagenbio-informatics.com/products/ingenuity-pathway-analysis).

Results

Cohort Characteristics

HIV-positive and HIV-negative cases from four sites in the National NeuroAIDS Tissue Consortium were combined to form a cohort of 34 HIV+ subjects and 24 HIV− controls. HIV+ subjects were further divided into groups with ($n = 18$) or without ($n = 16$) neurocognitive impairment (NCI), based on the available clinical data and neuropsychological evaluations. Demographics, clinical characteristics, and laboratory data are summarized in Table 1. HIV+ and HIV− groups were similar in age (median 54 and 58 years, respectively) and race (53% and 42% white), while the HIV+ group had more males (82% vs. 54%, $P = 0.04$). Illicit drug use ($P \leq 0.001$) and hepatitis C virus infection were more common in HIV+ subjects, and diabetes was more common in HIV− controls, while there was no significant difference in rates of hypertension, hyperlipidemia, body mass index, cancer history, cardiovascular disease, or cerebrovascular disease. Lack of available laboratory data in the control group precluded comparison with HIV+ cases. HIV+ subjects had a median of 19 [IQR 13–22] years duration of HIV infection prior to death; 100% were on HAART, with a perimortem median CD4 count of 283 [IQR 123–414] cells/μL (67% above 200 cells/μL), and the majority had undetectable plasma (62%) and cerebrospinal fluid (81%) viral loads at the last premortem study visit.

Premortem neurocognitive evaluations identified 18 HIV+ individuals with neurocognitive impairment, including five with HIV-associated dementia (HAD), two with mild neurocognitive disorder (MND), one with asymptomatic neurocognitive impairment (ANI), and ten with neuropsychological impairment attributed to other causes (NPI-O), while the remaining 16 HIV+ individuals were classified as unimpaired. Age, gender, race, duration of HIV infection, and CD4 counts were similar in HIV+ groups with vs. without NCI, but fewer NCI subjects were virally suppressed in plasma (50% vs. 81%, $P = 0.08$) or CSF (67% vs. 100%, $P = 0.1$). NCI subjects had higher rates of smoking, hypertension, hyperlipidemia, cancer, cardiovascular disease, and cerebrovascular disease, but there were no significant differences in illicit drug use, diabetes, or body mass index. Hepatitis C virus infections were more common in the no-NCI group (50% vs. 22%, $P = 0.01$), with corresponding elevations in median ALT and AST indicating liver dysfunction. Total cholesterol was slightly higher in the NCI group (181 vs. 141 mg/dL, $P = 0.04$), while there were no significant differences in HDL, LDL, or triglycerides. APOE genotyping revealed 10 subjects with at least one E4 allele, but no significant difference by neurocognitive status.

Neuropathologic Features

Postmortem evaluation was performed within 24 h of death in all but one case. There was no significant difference in postmortem interval between HIV+ and HIV− groups, or between HIV+ groups with and without NCI. The brain gross and histopathologic findings are summarized in Table 2. Inflammation, consisting predominantly of perivascular lymphocytes, mild lymphocytic or macrophage infiltrates, or occasional foci of macrophages/microglia, was reported in 29% of HIV+ subjects and none of the HIV− controls ($P = 0.009$). Reactive gliosis (41%, $P < 0.001$), myelin pallor (24%, $P = 0.02$), and microgliosis (12%, $P = 0.3$) were reported only in HIV+ subjects. Both HIV+ subjects and HIV− controls exhibited atherosclerosis, ischemic infarcts, Alzheimer type 2 astrogliosis, and non-HIV-associated neurodegenerative disease, with no significant differences between groups. Compared to subjects without NCI, HIV+ subjects with NCI had decreased gross brain weights (1270 vs. 1420 g, $P = 0.054$, when adjusted for gender), more reactive gliosis (67% vs. 13%, $P = 0.002$), and inflammation (44% vs. 13%, $P = 0.06$). Myelin pallor was identified only in HIV+ individuals with NCI (44% vs. 0%, $P = 0.003$). There were no significant differences in proportions of subjects with Alzheimer

Table 1 Characteristics of the study cohort

	HIV− (*n* = 24)	HIV+ (*n* = 34)	HIV+ no NCI (*n* = 16)	HIV+ NCI (*n* = 18)
Age at death (years), median [IQR]	58 [49–67]	54 [50–59]	52 [50–58]	56 [50–61]
Male gender, *n* (%)	13 (54)	28 (82)	15 (94)	13 (72)
White race, *n* (%)	10 (42)	18 (53)	10 (63)	8 (44)
PMI (h), median [IQR]	10 [7–17]	13 [8–18]	13 [6–16]	13 [8–19]
Smoking, *n* (%)	NA	15 (44)	5 (31)	10 (56)
Illicit drugs[a], *n* (%)	0 (0)	21 (62)	10 (63)	11 (61)
Hypertension, *n* (%)	4 (40)	9 (26)	2 (13)	7 (39)
Diabetes, *n* (%)	4 (40)	5 (15)	2 (13)	3 (17)
Hyperlipidemia, *n* (%)	4 (40)	11 (32)	3 (19)	8 (44)
Body mass index (kg/m^2), median [IQR]	27.9 [25.4–28.6]	22.9 [20.5–27.9]	23.7 [20.9–27.1]	22.9 [20.3–28.9]
Cancer[b], *n* (%)	3 (30)	12 (35)	4 (25)	8 (44)
Cardiovascular disease, *n* (%)	5 (50)	22 (65)	9 (56)	13 (72)
Cerebrovascular disease, *n* (%)	7 (44)	10 (29)	3 (19)	7 (39)
Hepatitis C virus infection positive, *n* (%)	1 (10)	12 (35)	8 (50)	4 (22)
FIB4[c] > 3.25, *n* (%)	NA	9 (36)	6 (60)	3 (20)
Creatinine (mg/dL), median [IQR]	NA	1.0 [0.8–1.3]	1.3 [0.7–1.4]	1.0 [0.8–1.2]
BUN (mg/dL), median [IQR]	NA	15 [11–19]	15 [12–19]	16 [11–20]
ALP (U/L), median [IQR]	NA	109 [92–150]	121 [98–148]	95 [84–153]
Albumin (g/dL), median [IQR]	NA	3.8 [2.9–4.3]	3.7 [2.7–4.2]	4.0 [3.6–4.3]
Total bilirubin (mg/dL), median [IQR]	NA	0.7 [0.4–1.3]	0.7 [0.4–1.3]	0.6 [0.3–1.2]
Total cholesterol (mg/dL), median [IQR]	NA	173 [140–187]	141 [110–172]	181 [169–207]
LDL (mg/dL), median [IQR]	NA	101 [92–118]	110 [73–114]	100 [95–117]
HDL (mg/dL), median [IQR]	NA	40 [35–44]	40 [37–43]	40 [31–51]
Triglycerides (mg/dL), median [IQR]	NA	169 [107–181]	167 [94–178]	172 [149–180]
APOE4 positive, *n* (%)	NA	10 (29)	6 (38)	4 (22)
Duration of HIV (years), median [IQR]	–	19 [13–22]	18 [12–22]	19 [15–22]
CD4 count (cells/μL), median [IQR]	–	283 [123–414]	306 [125–329]	277 [126–411]
CD4 < 200 cells/μL, *n* (%)	–	11 (33)	5 (33)	6 (33)
CD4 nadir (cells/μL), median [IQR]	–	98 [51–136]	70 [16–132]	99 [65–143]
Plasma VL (copies/mL), median [IQR]	–	40 [40–82]	40 [40–44]	53 [40–109]
Plasma VL < 50 copies/mL, *n* (%)	–	21 (62)	13 (81)	9 (50)
CSF VL (copies/mL), median [IQR]	–	40 [40–40]	40 [40–40]	40 [40–202]
CSF VL < 50 copies/mL, *n* (%)	–	17 (81)	9 (100)	8 (67)
HAART use, *n* (%)	–	34 (100)	16 (100)	18 (100)
Protease inhibitor use, *n* (%)	–	20 (59)	10 (63)	10 (56)
Neurocognitive impairment[d], *n* (%)	0 (0)	18 (53)	0 (0)	18 (100)

Abbreviations: *ALP* alkaline phosphatase, *APOE4* apolipoprotein E4, *BUN* blood urea nitrogen, *CSF* cerebrospinal fluid, *HAART* highly active antiretroviral therapy, *HDL* high-density lipoprotein, *IQR* interquartile range, *LDL* low-density lipoprotein, *NA* not available, *NCI* neurocognitive impairment, *PMI* postmortem interval, *VL* viral load

[a] Illicit drugs include cocaine, tetrahydrocannabinol, opioids, and stimulants

[b] Cancer diagnoses include lung carcinoma with brain metastases, lung carcinoma with epicardial metastases, colorectal carcinoma, gastric carcinoma, hepatocellular carcinoma (*n* – 2), lymphoma (*n* – 3), Kaposi's sarcoma, cancer not otherwise specified, gastrointestinal carcinoma not otherwise specified, myelodysplastic syndrome/leukemia, germ cell tumor with lung metastases, and carcinoid tumor

[c] Fibrosis 4 (FIB4) calculated from patient age, platelet count, and alanine aminotransferase and aspartate aminotransferase levels; score > 3.25 is 97% specific for advanced fibrosis with 65% positive predictive value

[d] Neurocognitive impairment diagnoses include one asymptomatic neurocognitive impairment (ANI), two mild neurocognitive disorder (MND), five HIV-associated dementia (HAD), and 10 neuropsychological impairment attributed to other causes (NPI-O)

Table 2 Brain gross and histopathologic features

	HIV− (n = 24)	HIV+ (n = 34)	P value	HIV+ no NCI (n = 16)	HIV+ NCI (n = 18)	P value
Inflammation	0 (0)	10 (29)	*0.009*	2 (13)	8 (44)	0.06
Reactive gliosis	0 (0)	14 (41)	*< 0.001*	2 (13)	12 (67)	*0.002*
AT2 astrocytosis	1 (5)	3 (9)	1.0	1 (6)	2 (11)	1.0
Microgliosis	0 (0)	4 (12)	0.3	2 (13)	2 (11)	1.0
Arteriosclerosis	5 (25)	6 (18)	0.7	2 (13)	4 (22)	0.7
Ischemic infarcts	4 (20)	6 (18)	1.0	1 (6)	5 (27)	0.2
Myelin pallor	0 (0)	8 (24)	*0.02*	0 (0)	8 (44)	*0.003*
Neoplasia	0 (0)	1 (3)	1.0	0 (0)	1 (6)	1.0
Neurodegenerative disease	2 (10)	2 (6)	0.6	0 (0)	2 (11)	0.5
Brain weight (g), median [IQR]	NA	1310 [1240–1420]	–	1420 [1290–1490]	1270 [1170–1380]	*0.02*
Brain RNA (cps/10^6 cells)a, median [IQR]	–	10.7 [2.6–38.0]	–	14.0 [2.3–30.6]	9.6 [2.8–52.8]	0.4
Brain DNA (cps/10^6 cells)a, median [IQR]	–	9.4 [5.4–19.4]	–	6.9 [3.8–25.2]	10.0 [8.3–15.7]	0.4

Abbreviations: *AT2* Alzheimer type II, *cps* copies, *IQR* interquartile range, *NCI* neurocognitive impairment

Data are n (%) unless otherwise indicated. Italicized values denote P value < 0.05 (Fisher's exact or Student's t test)

[a] Cell equivalents are based on hCCR5 with each diploid cell containing 2 copies of the hCCR5 gene [30]

type 2 astrogliosis, microgliosis, arteriosclerosis, or ischemic infarcts. Two HIV+ individuals with Alzheimer's disease-related neurodegenerative pathology and one subject with metastatic lung carcinoma exhibited NCI. Five subjects had an HIVE score of 2, including three individuals with microglial nodules, one with leukoencephalopathy, and one with lymphocytic inflammation.

HIV Brain Viral Loads

Single-copy HIV RNA and DNA VL assays detecting an HIV-1 gag target [29] were performed on frozen subcortical frontal white matter from HIV+ subjects. Values for HIV RNA and DNA VL (HIV gag copies normalized to 10^6 cell equivalents, based on 2 copies of hCCR5 per diploid cell) are summarized in Table 2. Among all HIV+ cases, median white matter HIV RNA VL was 10.7 [IQR 2.6–38.0] copies/10^6 cells and median HIV DNA VL was 9.4 [IQR 5.4–19.4] copies/10^6 cells. Individuals with non-suppressed plasma HIV RNA VL prior to death (> 50 copies/mL) had higher HIV DNA levels in postmortem frontal white matter tissue compared to those with suppressed plasma HIV RNA (P = 0.006), while no significant differences were observed in CSF or brain HIV RNA levels (Fig. 2a). Non-suppressed subjects with multiple elevated plasma and CSF HIV RNA VLs in the 10 years prior to death showed a trend towards higher white matter HIV RNA and DNA levels compared to those with durably suppressed plasma and CSF HIV RNA (Fig. 2b). There were no significant differences in white matter HIV DNA levels (10.0 vs. 6.9 copies/10^6 cells, P = 0.4) or HIV RNA levels (9.6 vs. 14.0 copies/10^6 cells, P = 0.4) between HIV+ subjects by NCI status (Table 2). Brain DNA viral load was higher for subjects with HIVE score 2 than for those with scores of 0 or 1 (median 25.0 vs. 8.8 cps/10^6 cells, P = 0.01), while there was no difference in RNA viral load (30.1 vs. 9.4 cps/10^6 cells, P = 0.7).

Gene Expression Profiling

Targeted gene expression profiling was performed on frozen white matter for 34 HIV+ and 24 HIV− subjects using NanoString nCounter technology. The workflow detailing the samples, probes, and analysis is illustrated in Fig. 1. A total of 933 unique probes were evaluated, which included genes related to inflammation/immune functions, stress responses, energy metabolism, and central nervous system function. The complete list of probes is listed in Table S2, and the set of genes used as cell-type markers (e.g., neuronal, astrocyte, myeloid, oligodendrocyte) is listed in Table S3.

Among 933 total gene probes, 800 genes shown in the volcano plot in Fig. 3a had sufficient signal above background levels and 325 probes produced sufficient signal and variance to warrant further analysis. Most differentially expressed genes showed modest fold changes (50 genes were differentially expressed with non-stringent FC > 1.3, P value < 0.1, FDR < 20%) primarily representing seven functional categories: interferon response, stress response, myeloid cells, major histocompatibility complex class 1 (MHC-1), T cells, oligodendrocytes, and energy metabolism (listed in Table S4). The majority of these genes showed increased expression in HIV+ subjects compared to HIV− controls. In contrast, expression of several oxidative phosphorylation/energy metabolism (PARK2, SREBF1, SREBF2, TXNIP) and oligodendrocyte (MAG, MOG) genes was decreased in HIV+ subjects. Given modest fold changes in differentially expressed genes, we used Pearson correlations to detect seven co-expression modules representing these functional categories and focused

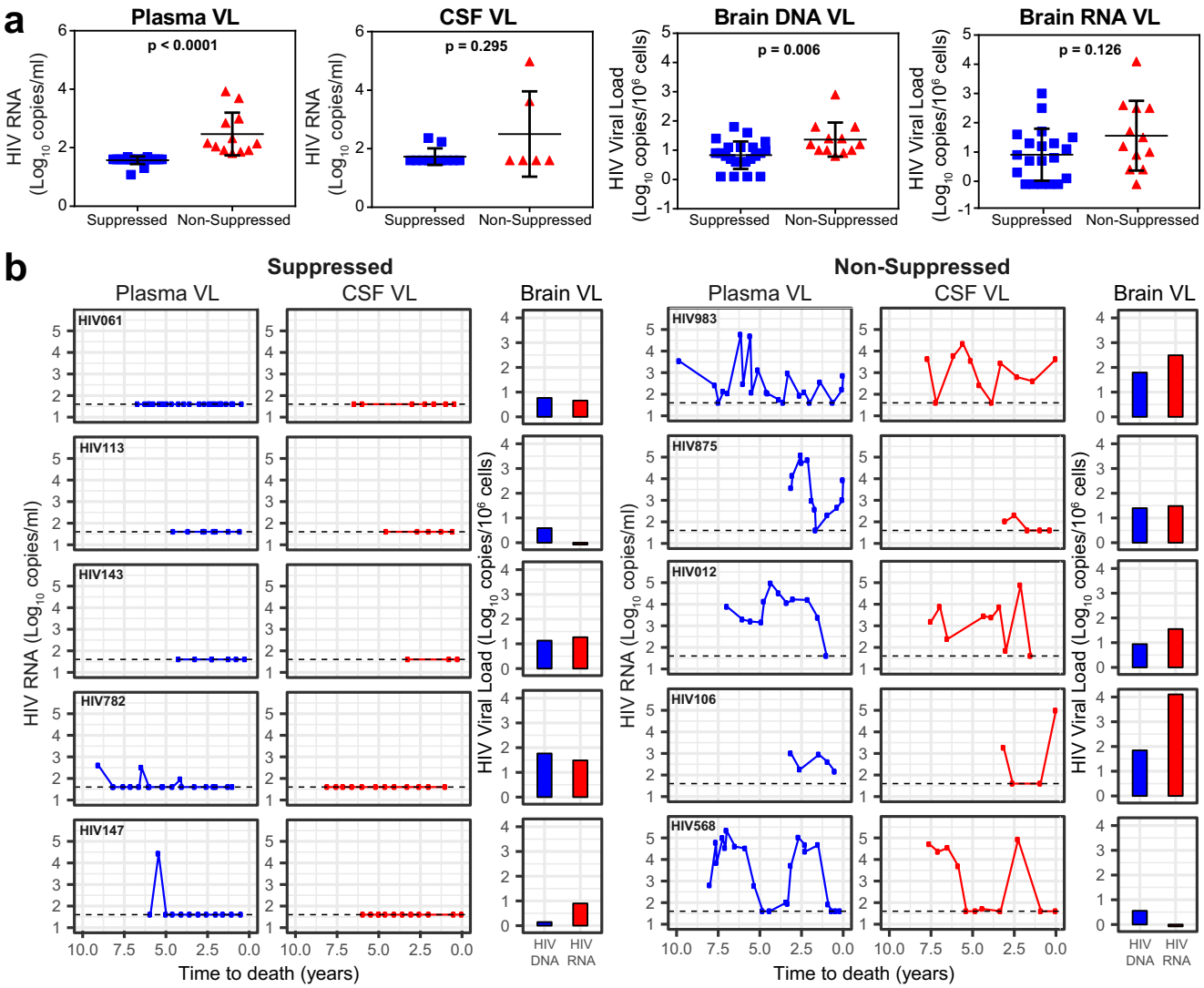

Fig. 2 Cerebrospinal fluid and brain viral loads in plasma-suppressed and non-suppressed HIV+ subjects. **a** Brain HIV DNA, but not brain HIV RNA or CSF viral loads (VL), was higher in individuals with detectable VL in plasma ($n = 12$) compared to individuals with undetectable plasma VL ($n = 22$; < 50 copies/mL). CSF viral loads were measured within the last 2 years prior to death. Medians and IQRs are indicated as horizontal and vertical lines, respectively. Statistical significance was calculated using the Mann-Whitney test. **b** Plasma and CSF HIV RNA, and post-mortem brain HIV DNA and RNA viral loads of representative plasma-suppressed ($n = 5$) and non-suppressed ($n = 5$) subjects. Blue and red solid lines in plasma and CSF panels, respectively, show viral load trajectories within 10 years prior to death. Horizontal dashed lines represent limit of assay detection (40 HIV RNA copies/mL)

subsequent analyses on 78 genes identified in these modules (Fig. 3b). As shown by the Pearson correlation coefficient matrix in Fig. 3b, interferon response, stress response, myeloid cell, MHC-1, and T cell genes correlated positively with each other, with the strongest correlations observed within each module. A subset of interferon response genes (IRF1, IRF7, IFITM2, IFI16, CGAS, NFKB2, STAT3) also correlated with the stress response gene module. Oxidative phosphorylation/energy metabolism and oligodendrocyte genes correlated positively with each other, but inversely with the other co-expression modules, suggesting decreased mitochondrial activity (oxidative phosphorylation/energy metabolism genes) and white matter integrity (oligodendrocyte genes) in the setting of increased inflammation (interferon response, MHC-1, myeloid, and T cell genes) and reactive oxygen species (stress response genes). None of these gene expression changes correlated with brain HIV RNA or DNA levels (data not shown). Gene expression was also compared between HIV+ NCI ($n = 18$) and no-NCI ($n = 16$) subjects, which identified only a trend towards differential expression of some interferon response-related genes (NLRC5, CXCL10, IRF7, STAT1, SIGLEC1, IFITM1 with $P < 0.1$). However, no genes met the criteria of FC > 1.3, P value < 0.1, FDR < 20% when we analyzed groups by NCI status (see Table S4).

Expression levels for the 78 genes belonging to co-expression modules are shown in a heatmap in Fig. 4. K-

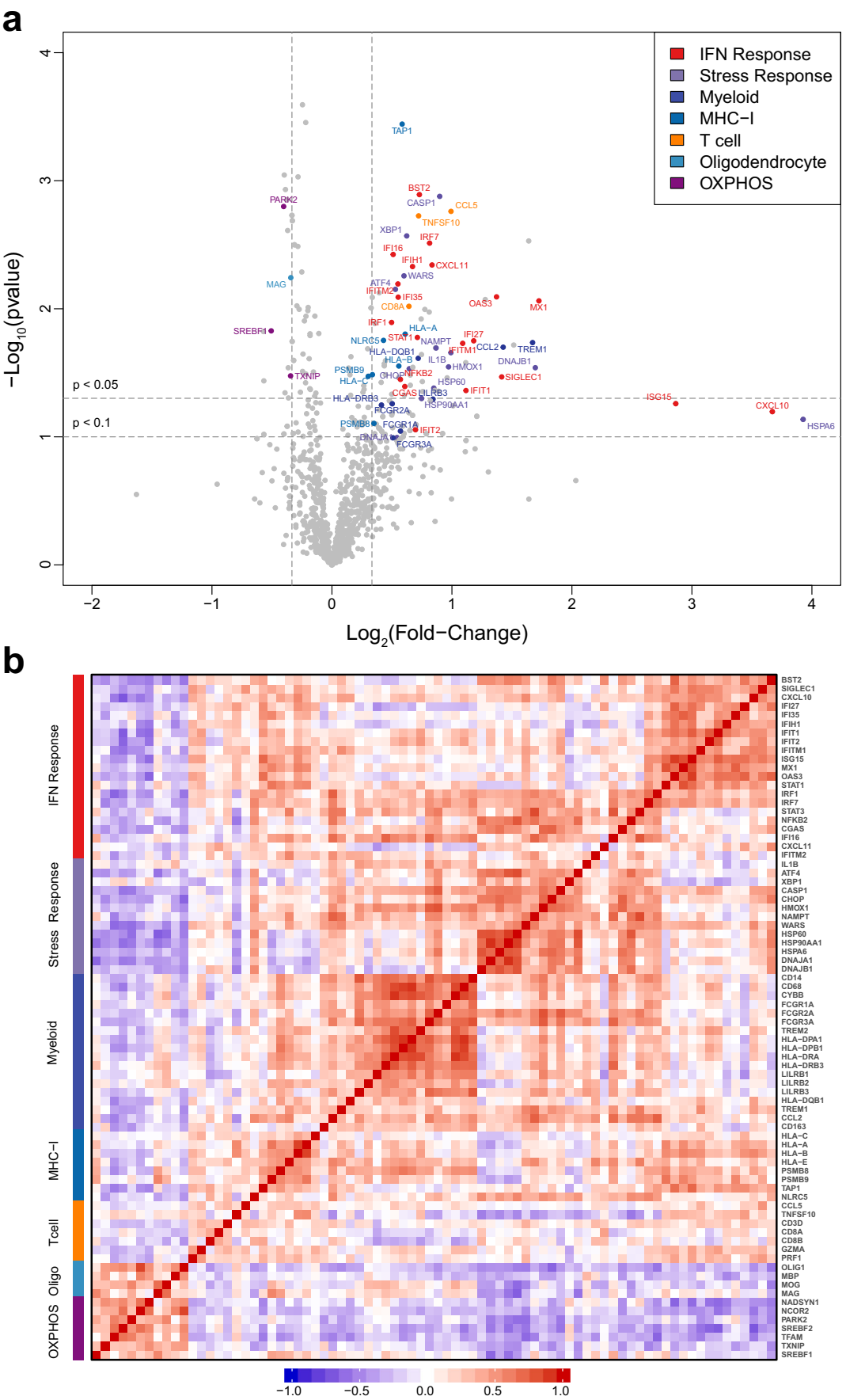
a
IFN Response
Stress Response
Myeloid
MHC−I
T cell
Oligodendrocyte
OXPHOS
−Log10(pvalue)
Log2(Fold−Change)
p < 0.05
p < 0.1
TAP1
BST2
PARK2
CASP1
CCL5
TNFSF10
XBP1
IRF7
IFI16
IFIH1
CXCL11
WARS
MAG
ATF4
IFITM2
IFI35
CD8A
OAS3
MX1
SREBF1
IRF1
HLA−A
STAT1
NLRC5
NAMPT
IFI27
CCL2
TREM1
HLA−DQB1
IFITM1
HLA−B
IL1B
DNAJB1
PSMB9
HMOX1
TXNIP
HLA−C
CHOP
NFKB2
SIGLEC1
HSP60
CGAS
LILRB3
IFIT1
HLA−DRB3
HSP90AA1
ISG15
CXCL10
FCGR2A
HSPA6
PSMB8
FCGR1A
IFIT2
DNAJA1
FCGR3A
b
IFN Response
Stress Response
Myeloid
MHC−I
Tcell
Oligo
OXPHOS
BST2
SIGLEC1
CXCL10
IFI27
IFI35
IFIH1
IFIT1
IFIT2
IFITM1
ISG15
MX1
OAS3
STAT1
IRF1
IRF7
STAT3
NFKB2
CGAS
IFI16
CXCL11
IFITM2
IL1B
ATF4
XBP1
CASP1
CHOP
HMOX1
NAMPT
WARS
HSP60
HSP90AA1
HSPA6
DNAJA1
DNAJB1
CD14
CD68
CYBB
FCGR1A
FCGR2A
FCGR3A
TREM2
HLA−DPA1
HLA−DPB1
HLA−DRA
HLA−DRB3
LILRB1
LILRB2
LILRB3
HLA−DQB1
TREM1
CCL2
CD163
HLA−C
HLA−A
HLA−B
HLA−E
PSMB8
PSMB9
TAP1
NLRC5
CCL5
TNFSF10
CD3D
CD8A
CD8B
GZMA
PRF1
OLIG1
MBP
MOG
MAG
NADSYN1
NCOR2
PARK2
SREBF2
TFAM
TXNIP
SREBF1
−1.0
−0.5
0.0
0.5
1.0

◀ **Fig. 3** Differential expression of genes in frontal lobe white matter in HIV+ subjects compared to age-matched controls. **a** Volcano plot shows genes differentially expressed in white matter between 34 HIV-positive versus 24 age-matched HIV-negative subjects. Labeled genes are differentially expressed based on low stringency cut-offs: FC > 1.3, $P < 0.1$, FDR < 20%. Dashed vertical lines represent fold change of 1.3 in either direction. **b** Pearson correlation matrix of r values for 78 genes from the 34 HIV-positive subjects mapped to the indicated co-expression modules. Colored bars to the left of the heatmap designate co-expression modules for each gene row. IFN, interferon; Oligo, oligodendrocyte; OXPHOS, oxidative phosphorylation/energy metabolism

means clustering identified three distinct subject clusters: cluster 1 (n = 11 HIV+ and 17 HIV− subjects) characterized by neutral or decreased expression of interferon response, stress response, and MHC-1 genes; variable expression of myeloid cell and T cell genes; and increased expression of oligodendrocyte and energy metabolism genes; cluster 2 (n = 15 HIV+ and 7 HIV− subjects) characterized by mild to moderately increased expression of interferon response, stress response, myeloid cells, MHC-1 upregulation, and T cell genes, and variable expression of oligodendrocyte and energy metabolism genes; and cluster 3 (n = 8 HIV+ and 0 HIV− subjects) characterized by markedly increased expression of interferon response, stress response, myeloid cell, MHC-1, and T cell genes, and decreased expression of oligodendrocyte and energy metabolism genes. Cluster 3 also contained all of the cases with high levels of CNS inflammation (HIVE score = 2) and a preponderance of subjects with NCI (6/8, 75%), non-suppressed plasma HIV VL (75%), brain HIV DNA VL > 10 copies/10^6 cells (50%), and at least one APOE4 allele (50%). Subjects in this cluster were characterized by histological and gene expression evidence of inflammation and myelin disruption, and gene expression evidence of increased stress response and decreased mitochondrial function. Among HIV+ subjects in clusters 1 and 2, there was no significant difference in any covariates evaluated, including plasma HIV RNA VL, brain HIV DNA VL, NCI status, cerebrovascular disease, APOE genotypes, or HIVE score. There was no significant difference in the proportion of subjects over 60 years of age between the three clusters.

Network Analysis

IPA identified three high-scoring networks shown in Fig. 5a–c for 33 of the top 40 differentially expressed genes shown in Fig. 5d. The interferon response network included key genes associated with interferon-related antiviral functions including recognition of viral nucleic acids (IFIT1, IFIT2, CGAS, IFI16, IFIH1), inhibition of virus fusion or diffusion within cellular membranes (BST2, IFITM1, IFITM2), and cell signaling and/or transcriptional regulation (STAT1, STAT3, IRF1, IRF7). Four of the most strongly upregulated genes in HIV+ subjects in this network were interferon response genes ISG15 (ubiquitin-like modifier with multiple functions including blocking HIV replication and virus release), MX1 (GTPase that blocks endocytic trafficking of viral components), OAS3 (producer of 2′–5′ oligoadenylates which activate RNase L), and IFI27 (mitochondria-associated pro-apoptotic protein) [34–37]. STATs, IRF1, IRF7, and IFI16 were identified as key transcriptional regulators in this network. A second network of MHC class 1-associated genes was upregulated in HIV+ subjects, which included HLA-A, HLA-B, and HLA-C, regulators of MHC-1 gene expression (NLRC5), transportation of virus peptides (TAP1), and immunoproteasome subunits (PSMB8, PSMB9). A third interconnected network included stress response and oxidative phosphorylation/energy metabolism genes, including upregulated genes involved in the unfolded protein response and apoptosis (XBP1, CASP1, CHOP, ATF4) and downregulated genes involved in lipid homeostasis (SREBF1, SREBF2), autophagy of damaged mitochondria (PARK2), and inhibition of antioxidation (TXNIP). These network models identified several key transcription factors with altered expression levels, including IRF1, IRF7, IFI16, STAT1, STAT3, NLRC5, XBP1, ATF4, CHOP, SREBF1, and SREBF2, consistent with a robust cellular response to HIV infection.

Validation of Differentially Expressed Genes and SVM-Based 15-Gene Signature

Differentially expressed genes identified in the preceding analyses (34 HIV+ vs. 24 HIV−) were tested for differential expression against independent microarray datasets published by Borjabad et al. (6 HIV+ on HAART vs. 6 HIV−) and Gelman et al. (14 HIV+ on HAART vs. 6 HIV−) [13, 14]. Twenty-two differentially expressed genes identified in the present study were also upregulated in at least one of the other studies, listed in Supplementary Tables S5 and S6. These genes were predominantly associated with interferon responses (n = 13), but also included stress response (n = 4) and MHC-1 (n = 4) genes, and TNFSF10. None of the downregulated oligodendrocyte or oxidative phosphorylation genes were identified in the studies by Borjabad et al. or Gelman et al., which may reflect greater statistical power in the present study due to more HIV+ subjects and HIV− controls, younger age of subjects in these prior studies (median age 45 years vs. 54 years in our study cohort) [14], or earlier calendar period of the prior studies, which impacts availability of newer antiretroviral drugs [13, 14].

Support vector machine (SVM) learning identified a core signature of 15 genes with high predictive accuracy for predicting HIV status, consisting of genes related to interferon responses (CXCL10, IFITM1, IRF7, ISG15, MX1, OAS3), stress responses (ATF4, XBP1, CASP1, WARS), MHC-1 (HLA-A, HLA-B, TAP1), and T cells (CCL5, TNFSF10). Using fivefold and threefold cross-validation to test prediction

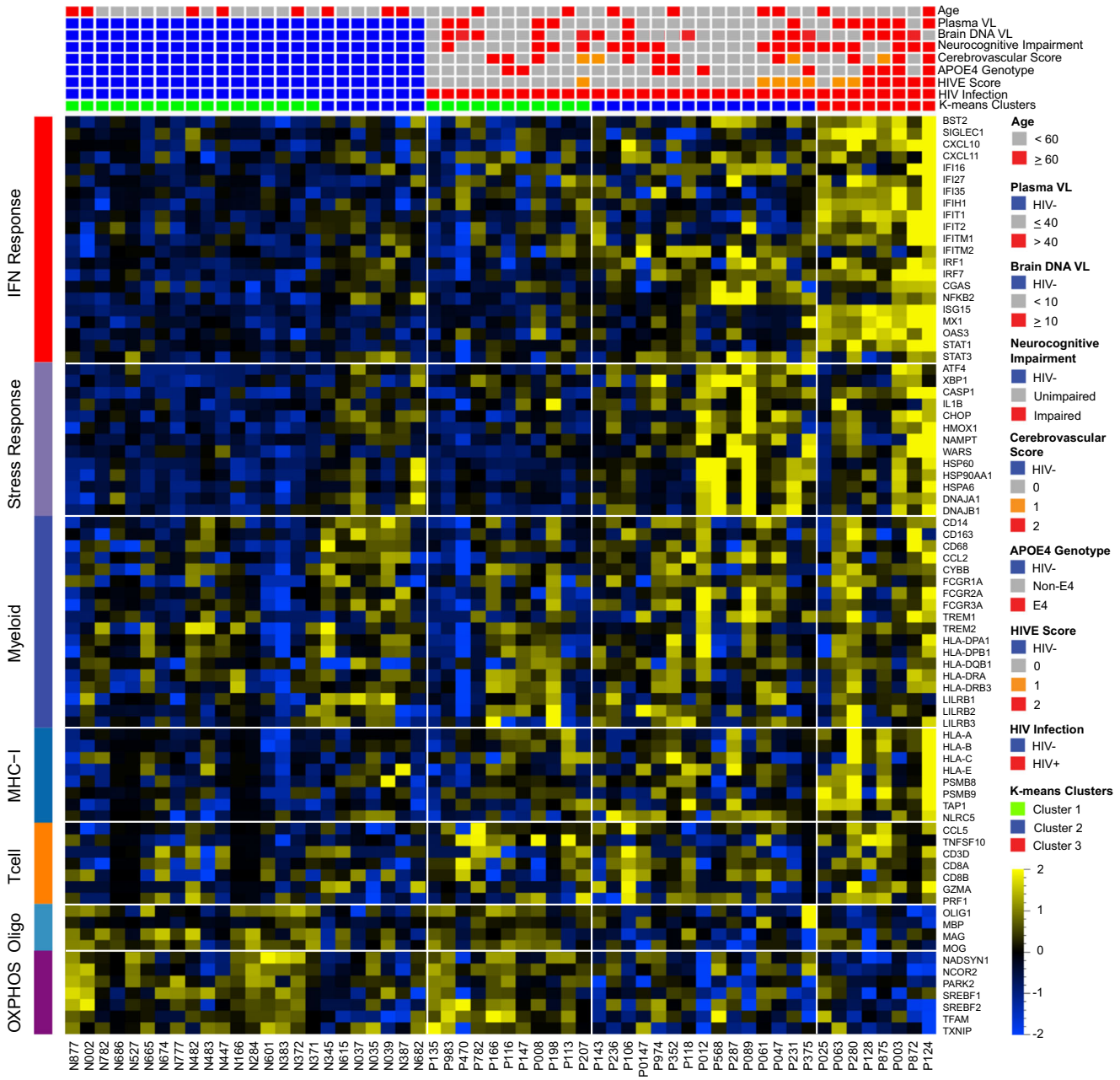

Fig. 4 Gene expression heatmap of white matter gene expression changes in HIV+ subjects and age-matched controls. K-means clustering of white matter gene expression for genes in co-expression modules shown in Fig. 3b identified three subject clusters in the HIV+ cohort. Colored bars above the heatmap show covariate values for each subject column. Colored bars to the left of the heatmap designate co-expression modules for each gene row

accuracy on training (n = 58) and validation (n = 12) sets, respectively, HIV+ and HIV− subjects were identified with 82% and 79% accuracy, respectively, in the training set (mean 81% accuracy) and 86% and 83% accuracy, respectively, in an independent test set (mean 85% accuracy) of HAART-treated HIV+ and HIV− white matter samples from the study by Borjabad et al. [14]. These 15 genes were significantly upregulated in HAART-treated HIV+ subjects compared to HIV− controls ($P < 0.05$), regardless of white matter HIV DNA VL above or below 10 copies/10^6 cells (Fig. 6). Furthermore, Supplementary Tables S5 and S6 show that 14 of these 15 genes were upregulated in one or both studies by Borjabad et al. or Gelman et al. [13, 14].

Discussion

This is the largest study to date of gene expression profiling of brain tissue from HIV+ patients on HAART. Consistent with prior studies [13, 14], interferon response genes were among

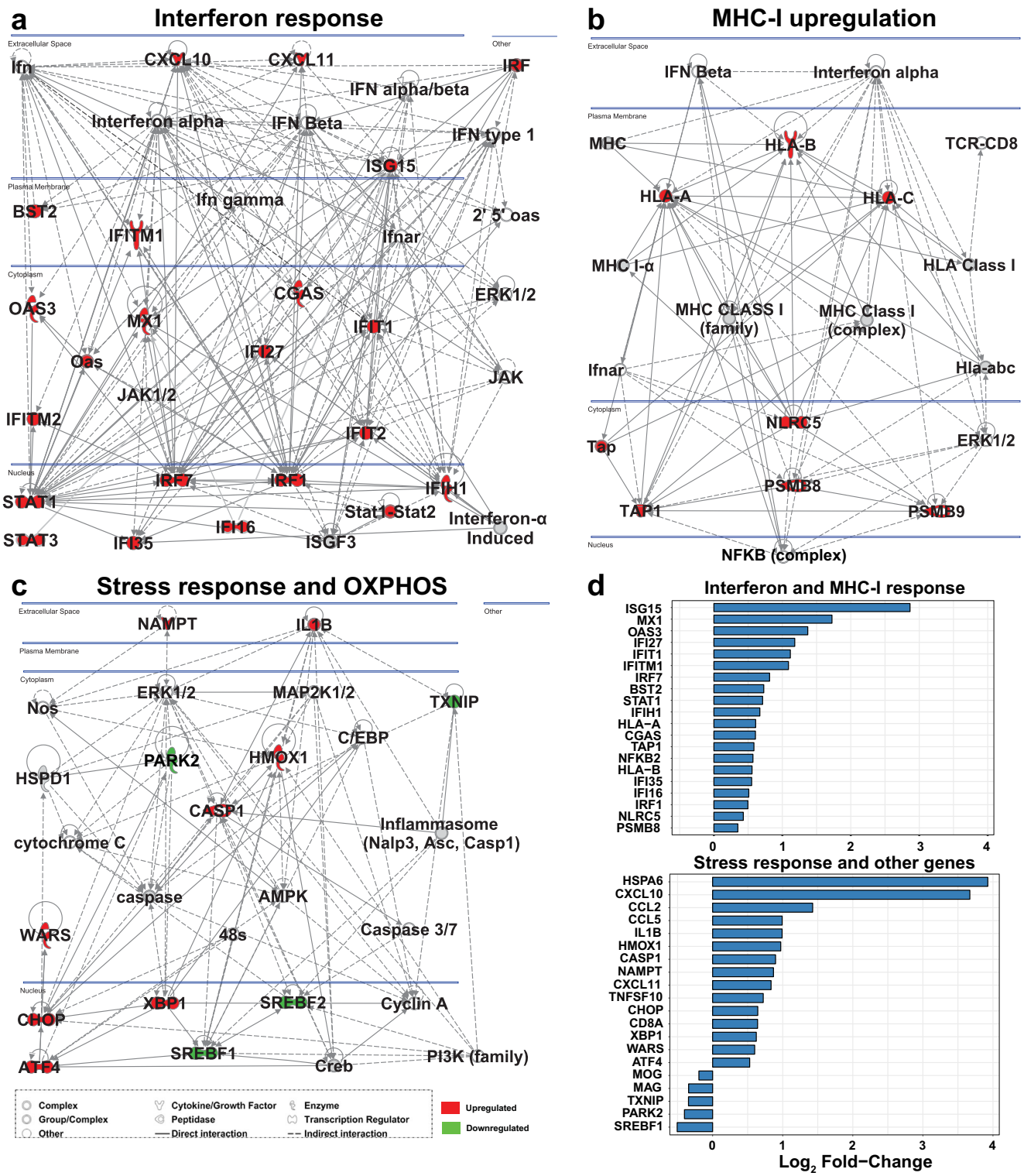

Fig. 5 High-scoring networks for differentially expressed genes mapping to interferon response, MHC-1 upregulation, stress response, and oxidative phosphorylation/energy metabolism. Network diagrams of **a** interferon response, **b** MHC-I upregulation, and **c** stress response and oxidative phosphorylation (OXPHOS) generated by Ingenuity Pathway Analysis software show interactions (edges) between genes (nodes). Nodes highlighted red or green are differentially expressed (FC > 1.3, $P < 0.05$, FDR < 10%) for 34 HIV+ and 24 age-matched HIV− controls. **d** Barplots of 40 differentially expressed genes (FC > 1.2, $P < 0.1$, FDR < 10%) in HIV+ vs. HIV-negative controls, including interferon and MHC-1 response (top) and stress response genes (bottom), 33 of which are highlighted in network diagrams in panels **a**–**c**

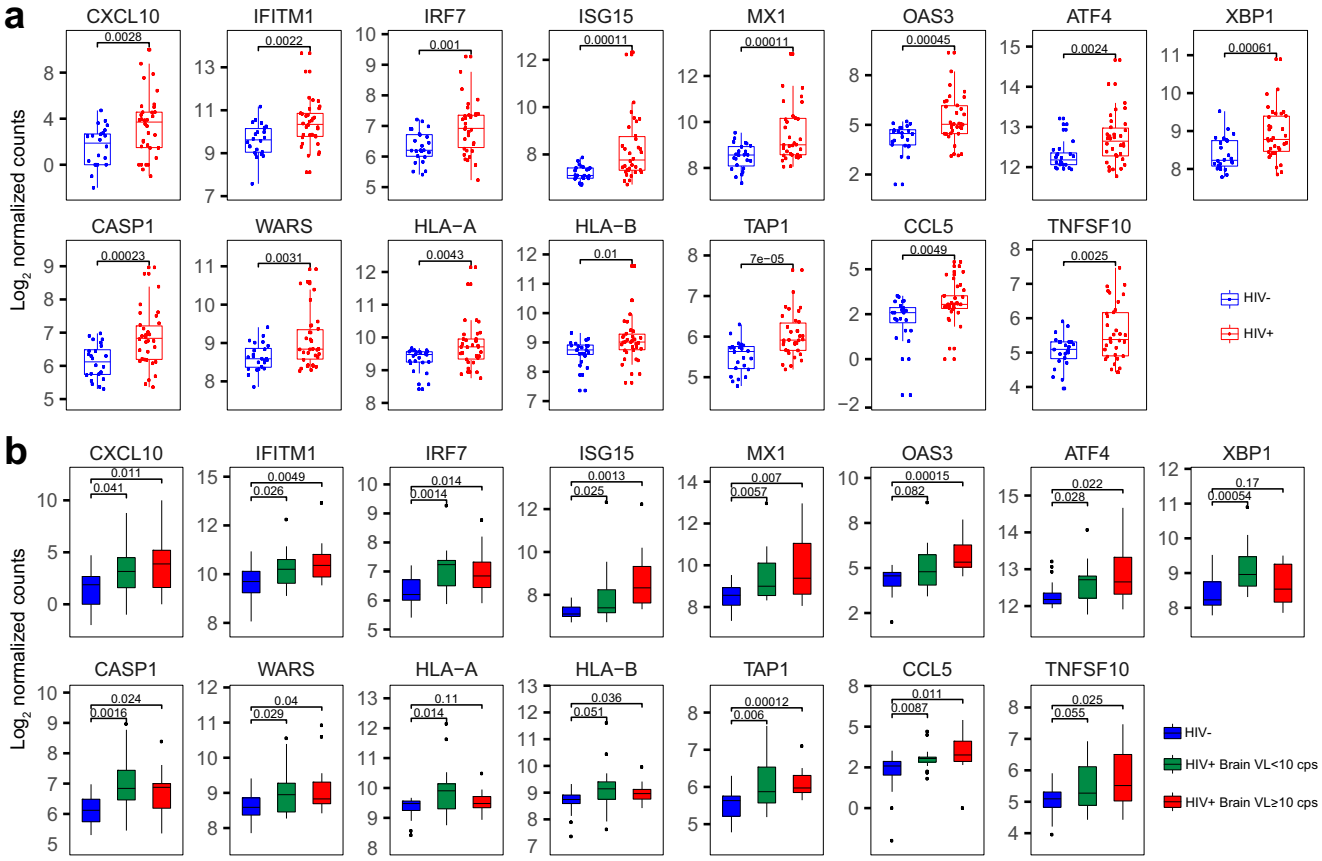

Fig. 6 Expression levels of a 15-gene signature predictive of HIV status. Boxplots show expression levels for each gene in the 15-gene signature discovered by support vector machine learning. Differential expression in **a** HIV+ subjects versus age-matched HIV− controls or **b** HIV+ subjects stratified by HIV brain DNA VL < 10 copies/10^6 cells or ≥ 10 copies/10^6 cells versus age-matched HIV− controls ($P < 0.05$). Horizontal bars represent medians, boxes span the interquartile range (IQR), and whiskers extend to extreme data points within 1.5 times the IQR. *P* values calculated using Welch's *t* test ($n = 24$ HIV−, $n = 14$ HIV+ subjects with brain DNA VL < 10 copies/10^6 cells, $n = 18$ HIV+ subjects with brain DNA VL ≥ 10 copies/10^6 cells)

the most strongly upregulated genes in HIV+ subjects compared to HIV− controls, reflecting activation of the immune system in response to ongoing viral infection. Stress response-, myeloid, MHC-1-, and T cell-associated genes were also upregulated in HIV+ subjects, while oligodendrocyte and energy metabolism genes were downregulated. Machine learning identified a 15-gene signature, comprised of interferon response-, stress response-, MHC-1-, and T cell-associated genes, which predicted HIV status with 81% accuracy in the training set and 85% accuracy in an independent test set from HAART-treated HIV+ subjects and HIV− controls [14]. The increase in immune response gene expression had a clear histopathological correlate in many cases, consisting of perivascular and parenchymal immune cell infiltrates (29% HIV+ vs. 0% HIV−, $P = 0.009$). Similarly, myelin pallor, an expected correlate of decreased oligodendrocyte gene expression [19], was observed in 24% of HIV+ subjects (all with NCI) and no controls ($P = 0.02$). Additional nonspecific histopathological abnormalities were observed in HIV+ subjects, including reactive gliosis, Alzheimer type 2 astrocytosis, microgliosis, ischemic infarcts, neoplasia, and neurodegenerative disease. NCI was more frequently associated with inflammation ($P = 0.06$), myelin pallor ($P = 0.003$), and reactive gliosis ($P = 0.002$), despite no differences in duration of HIV infection, CD4 counts, or HIV DNA or RNA levels in postmortem brains. NCI+ and NCI− groups showed no significant differences in age, gender, race, and several comorbidities including illicit drug use and diabetes. Despite histological differences between HIV+ subjects with and without NCI, we did not identify differentially expressed genes that reliably distinguished between HIV+ individuals with or without NCI by fold-change analysis, k-means clustering, or principal component analysis (Fig. 4, Table S4, and data not shown). Several interferon response genes (i.e., CXCL10, IRF7, STAT1, SIGLEC1, and IFITM1) exhibited a trend towards increased expression in HIV+ subjects with NCI, consistent with an inflammatory subtype of HAND. However, no genes were statistically significant after correction for multiple testing (FDR > 20%).

White matter abnormalities are a critical component in HAND pathogenesis, supported in our study by decreased

expression of oligodendrocyte-associated genes including OLIG1, MBP, MAG, and MOG. Oligodendrocytes synthesize lipids and proteins to generate and maintain myelin, with additional lipids synthesized by astrocytes and transported by apolipoprotein E [38, 39]. The APOE4 allele has a diminished capacity for lipid transport, and has been associated with reduced white matter intensity and decreased cognitive performance in older HIV+ individuals [40]. APOE4 was present in 50% of k-means cluster 3 subjects, a group enriched for white matter inflammation and NCI (Fig. 4), which also exhibited the most prominent downregulation of oligodendrocyte-associated genes. In models of multiple sclerosis, cholesterol-synthesis pathways are markedly upregulated in oligodendrocytes during remyelination [39]. Conversely, sterol regulatory element binding transcription factor 1 (SREBF1) and SREBF2, transcription factors that regulate cholesterol and fatty acid genes [41], were decreased in HIV+ white matter in the present study. Oligodendrocytes have been shown to decrease with age [19], a process that may be accelerated by HIV infection and concurrent cerebrovascular or metabolic disease.

While the dense inflammatory infiltrate and multinucleated giant cells of HIVE are not present in HIV+ patients on HAART, microgliosis and lymphocytic infiltration are recurrent histological findings that contribute to NCI [11]. Inflammation is typically attributed to a direct response to HIV virions or components; however, inflammatory changes can also be detected in the absence of productive viral replication and microgliosis has been associated with some antiretroviral drugs [17]. Prior gene expression studies and meta-analyses in HIV+ subjects identified differentially expressed genes associated with interferon response, antigen processing, and cytokine signaling [13, 14, 42]. Similar pathways are active in aging and other neurological/neurodegenerative disorders, raising the possibility of an accelerated aging mechanism [10, 43, 44]. In this study, several interferon response genes, including ISG15, MX1, IFI16, CGAS, and OAS3, were upregulated in HIV+ individuals compared to negative controls (Fig. 5a). Interferon gamma-inducible protein 16 (IFI16), through binding of dsDNA, is responsible for recruitment and activation of TANK-binding kinase 1 in the stimulator of interferon genes (STING) complex and cyclic GMP-AMP synthase (CGAS) [45–47]. Following HIV infection, 2′–5′-oligoadenylate synthetase genes, such as OAS3, have been shown to be upregulated in response to monocyte-derived interferon, without normalization after initiation of HAART [48]. Taken together, these findings support chronic immune activation and persistent interferon response as a prominent feature and likely instigator of some forms of HAND.

Oxidative phosphorylation is the major source of energy in the brain, which has increased energy demands in the setting of HIV-triggered chronic inflammation [49]. The accumulation of excess reactive oxygen species leads to oxidative stress, implicated in many neurological diseases. Downregulation of several oxidative phosphorylation/energy metabolism-associated genes was observed in HIV+ subjects, including PARK2, TFAM, and SREBF1, with concurrent upregulation in stress response genes including ATF4, XBP1, CHOP, CASP1, and IL1-β (Fig. 5c). Diminished PARK2 expression (encoding the E3 ubiquitin ligase Parkin) leads to increased activation of endothelial nitric oxide synthase (eNOS) and enhanced levels of reactive oxygen species and mitochondrial dysfunction [50, 51]. While predominantly expressed in neurons, PARK2 has recently been shown to co-localize in white matter astrocytes in multiple sclerosis lesions [52]. Transcriptional factor A (TFAM) protects mitochondrial DNA by binding and preventing damage by reactive oxygen species, and decreased TFAM activity may contribute to several neurodegenerative diseases [26, 53]. Thioredoxin interacting protein (TXNIP) has been reported to increase inflammatory responses in stroke and Alzheimer's disease via activation of the NOD-like receptor protein (NLRP3)-inflammasome, and has been proposed as a possible therapeutic target for multiple neurological diseases involving grey and white matter [54]. NLRP3 expression was increased in antiretroviral-treated non-responders (CD4 ≤ 350 cells/μL) compared to responders [55], and the decreased expression of TXNIP in HIV+ subjects observed here may indicate a mechanism for decreased NLRP3 expression. SREBF1 regulates cholesterol and fatty acid gene expression, is critical for myelination, and has also been implicated in lipid-mediated cellular stress [38, 41, 56]. Activating transcription factor 4 (ATF4), a transcriptional regulator involved in autophagy, oxidative stress, and inflammation, has also been shown to be increased in AD and PD [57]. Caspase-1 and IL-1β are associated with apoptosis and inflammatory responses, and remain elevated in SIV infection despite HAART treatment [58]. Dysregulation of oxidative phosphorylation and stress response has a clear role in cellular dysfunction and death, and appears to contribute to HIV-associated white matter abnormalities.

Taken together, the clinical, laboratory, histological, and gene expression data suggest a model in which chronic HIV infection and multiple comorbidities lead to cognitive deficits due in part to white matter damage. In HIV+ individuals, expression of inflammation and stress response genes is increased, while expression of oxidative phosphorylation genes is decreased, consistent with a model in which chronic inflammation and decreased mitochondrial function may both contribute to generation of increased reactive oxygen species (ROS) and stress responses. Increased ROS may further contribute to mitochondrial dysfunction by damaging mitochondrial DNA. Oligodendrocytes are particularly vulnerable to oxidative damage, providing a potential explanation for inflammation-mediated myelin pallor, which along with

arteriosclerosis and vascular compromise leads to white matter damage and neurological dysfunction. Comorbidities including vascular, neurodegenerative, and systemic/metabolic diseases are all expected to exacerbate the primary effects of HIV infection. Given this scenario, therapies that decrease chronic inflammation while promoting mitochondrial integrity may help to preserve white matter integrity in older HIV+ individuals.

Limitations of this study include heterogeneity of the study cohort, incomplete clinical and laboratory data, and quantity of postmortem tissue available. HIV+ subjects in the study cohort originated from four NNTC sites across the USA, had a median age of 54 years and median duration of HIV infection of 19 years, and had autopsies performed between 2000 and 2014. Therefore, study subjects received many different antiretroviral drug regimens. The sensitivity of HIV testing increased over time, and earlier cases reported as undetectable may have been reclassified as low positive with more sensitive current assays. While a large amount of clinical and laboratory information was available for these subjects, significant gaps remained, including lack of laboratory data for the majority of HIV-negative controls, raising the possibility that certain associations may be under- or over-estimated. For brain HIV VL testing and gene expression profiling, only a single anatomical site was tested for each subject, which can lead to sampling bias and precludes the ability to detect regional differences. Confirming these results in the temporal lobe, given its prominent roles in neurodegenerative disease (e.g., Alzheimer's disease), viral infections (e.g., herpes simplex encephalitis), and aging, would be of particular interest. The NanoString platform offers significant flexibility in designing panels of probe targets, but has a lower dynamic range compared to RNAseq. Due to cellular heterogeneity of brain tissue, it remains difficult to distinguish changes specific to any particular cell type, which could be addressed with single cell sequencing in future studies [59, 60].

Conclusions

This is the largest study to date to evaluate gene expression changes in frontal lobe white matter in HIV+ individuals on HAART. White matter dysfunction has emerged as a key component of normal aging and in neurodegenerative diseases, and our study supports a critical role in HIV pathogenesis in the brain of virally suppressed subjects. Differentially expressed genes were identified and mapped into pathways and networks, and a core signature predicting HIV status was identified and validated using results from prior studies. These findings confirm the critical role of interferon response-, stress response-, energy metabolism-, MHC-1-, T cell-, myeloid-, and oligodendrocyte-associated genes in HAND pathogenesis. No differentially expressed genes or specific patterns distinguished HIV+ subjects by cognitive status, possibly reflecting heterogeneous subtypes within the NCI+ group, many of which were NPI-O rather than HAND. Further studies with larger cohorts of individuals who have neuropsychologically confirmed impairment, multiple anatomic sites, and evaluation of specific cell types at the single-cell level will aid in better understanding of the cellular pathways involved and may lead to identification of drug targets or modifiable risk factors to preserve white matter integrity and cognitive function in the aging HIV+ population.

Acknowledgments We thank the Dana-Farber/Harvard Cancer Center Molecular Biology Core for the NanoString nCounter platform services. This work was supported by National Institutes of Health grants to D.G. (R01 MH097659 and R01 DA40391). Financial support for the NNTC was provided through the following cooperative agreements from the National Institutes of Health: U24MH100930, U24MH100931, U24MH100928, U24MH100929, and U24MH100925. This study was supported in part with federal funds from the National Cancer Institute, National Institutes of Health, under contract no. HSN261200800001E. The content of this publication does not necessarily reflect the views or policies of the Department of Health and Human Services, nor does mention of any trade names, commercial products, or organizations imply endorsement by the US government.

References

1. Sacktor N (2018) Changing clinical phenotypes of HIV-associated neurocognitive disorders. J Neurovirol 24(2):141–145. https://doi.org/10.1007/s13365-017-0556-6
2. Eggers C, Arendt G, Hahn K, Husstedt IW, Maschke M, Neuen-Jacob E, Obermann M, Rosenkranz T et al (2017) HIV-1-associated neurocognitive disorder: epidemiology, pathogenesis, diagnosis, and treatment. J Neurol 264(8):1715–1727. https://doi.org/10.1007/s00415-017-8503-2
3. Saylor D, Dickens AM, Sacktor N, Haughey N, Slusher B, Pletnikov M, Mankowski JL, Brown A et al (2016) HIV-associated neurocognitive disorder–pathogenesis and prospects for treatment. Nat Rev Neurol 12(4):234–248. https://doi.org/10.1038/nrneurol.2016.27
4. Geffin R, McCarthy M (2018) Aging and apolipoprotein E in HIV infection. J Neurovirol 24(5):529–548. https://doi.org/10.1007/s13365-018-0660-2
5. Lamers SL, Rose R, Maidji E, Agsalda-Garcia M, Nolan DJ, Fogel GB, Salemi M, Garcia DL et al (2016) HIV DNA is frequently present within pathologic tissues evaluated at autopsy from combined antiretroviral therapy-treated patients with undetectable viral loads. J Virol 90(20):8968–8983. https://doi.org/10.1128/JVI.00674-16
6. Ko A, Kang G, Hattler JB, Galadima HI, Zhang J, Li Q, Kim WK (2019) Macrophages but not astrocytes harbor HIV DNA in the brains of HIV-1-infected aviremic individuals on suppressive antiretroviral therapy. J Neuroimmune Pharmacol 14(1):110–119. https://doi.org/10.1007/s11481-018-9809-2
7. Mackiewicz MM, Overk C, Achim CL, Masliah E (2019) Pathogenesis of age-related HIV neurodegeneration. J Neurovirol.:1–12. https://doi.org/10.1007/s13365-019-00728-z

8. Cysique LA, Brew BJ (2019) Vascular cognitive impairment and HIV-associated neurocognitive disorder: a new paradigm. J Neurovirol.:1–12. https://doi.org/10.1007/s13365-018-0706-5
9. Ulfhammer G, Eden A, Mellgren A, Fuchs D, Zetterberg H, Hagberg L, Nilsson S, Yilmaz A et al (2018) Persistent central nervous system immune activation following more than 10 years of effective HIV antiretroviral treatment. AIDS 32(15):2171–2178. https://doi.org/10.1097/QAD.0000000000001950
10. Cribbs DH, Berchtold NC, Perreau V, Coleman PD, Rogers J, Tenner AJ, Cotman CW (2012) Extensive innate immune gene activation accompanies brain aging, increasing vulnerability to cognitive decline and neurodegeneration: a microarray study. J Neuroinflammation 9:179. https://doi.org/10.1186/1742-2094-9-179
11. Tavazzi E, Morrison D, Sullivan P, Morgello S, Fischer T (2014) Brain inflammation is a common feature of HIV-infected patients without HIV encephalitis or productive brain infection. Curr HIV Res 12(2):97–110
12. Raj D, Yin Z, Breur M, Doorduin J, Holtman IR, Olah M, Mantingh-Otter IJ, Van Dam D et al (2017) Increased white matter inflammation in aging- and Alzheimer s disease brain. Front Mol Neurosci 10:206. https://doi.org/10.3389/fnmol.2017.00206
13. Gelman BB, Chen T, Lisinicchia JG, Soukup VM, Carmical JR, Starkey JM, Masliah E, Commins DL et al (2012) The National NeuroAIDS Tissue Consortium brain gene array: two types of HIV-associated neurocognitive impairment. PloS one 7(9):e46178. https://doi.org/10.1371/journal.pone.0046178
14. Borjabad A, Morgello S, Chao W, Kim SY, Brooks AI, Murray J, Potash MJ, Volsky DJ (2011) Significant effects of antiretroviral therapy on global gene expression in brain tissues of patients with HIV-1-associated neurocognitive disorders. PLoS Pathog 7(9): e1002213. https://doi.org/10.1371/journal.ppat.1002213
15. Shah A, Gangwani MR, Chaudhari NS, Glazyrin A, Bhat HK, Kumar A (2016) Neurotoxicity in the post-HAART era: caution for the antiretroviral therapeutics. Neurotox Res 30(4):677–697. https://doi.org/10.1007/s12640-016-9646-0
16. Gullett JM, Lamb DG, Porges E, Woods AJ, Rieke J, Thompson P, Jahanshad N, Nir TM et al (2018) The impact of alcohol use on frontal white matter in HIV. Alcohol Clin Exp Res 42(9):1640–1649. https://doi.org/10.1111/acer.13823
17. Soontornniyomkij V, Umlauf A, Soontornniyomkij B, Gouaux B, Ellis RJ, Levine AJ, Moore DJ, Letendre SL (2018) Association of antiretroviral therapy with brain aging changes among HIV-infected adults. AIDS 32(14):2005–2015. https://doi.org/10.1097/QAD.0000000000001927
18. Su T, Wit FW, Caan MW, Schouten J, Prins M, Geurtsen GJ, Cole JH, Sharp DJ et al (2016) White matter hyperintensities in relation to cognition in HIV-infected men with sustained suppressed viral load on combination antiretroviral therapy. AIDS 30(15):2329–2339. https://doi.org/10.1097/QAD.0000000000001133
19. Hase Y, Horsburgh K, Ihara M, Kalaria RN (2018) White matter degeneration in vascular and other ageing-related dementias. J Neurochem 144(5):617–633. https://doi.org/10.1111/jnc.14271
20. Sanford R, Strain J, Dadar M, Maranzano J, Bonnet A, Mayo NE, Scott SC, Fellows LK et al (2019) HIV infection and cerebral small vessel disease are independently associated with brain atrophy and cognitive impairment. AIDS 33(7):1197–1205. https://doi.org/10.1097/QAD.0000000000002193
21. Underwood J, Cole JH, Caan M, De Francesco D, Leech R, van Zoest RA, Su T, Geurtsen GJ et al (2017) Gray and white matter abnormalities in treated human immunodeficiency virus disease and their relationship to cognitive function. Clin Infect Dis 65(3): 422–432. https://doi.org/10.1093/cid/cix301
22. Kuhn T, Kaufmann T, Doan NT, Westlye LT, Jones J, Nunez RA, Bookheimer SY, Singer EJ et al (2018) An augmented aging process in brain white matter in HIV. Hum Brain Mapp 39(6): 2532–2540. https://doi.org/10.1002/hbm.24019
23. Everall I, Vaida F, Khanlou N, Lazzaretto D, Achim C, Letendre S, Moore D, Ellis R et al (2009) Cliniconeuropathologic correlates of human immunodeficiency virus in the era of antiretroviral therapy. J Neurovirol 15(5-6):360–370. https://doi.org/10.3109/13550280903131915
24. Solomon IH, De Girolami U, Chettimada S, Misra V, Singer EJ, Gabuzda D (2017) Brain and liver pathology, amyloid deposition, and interferon responses among older HIV-positive patients in the late HAART era. BMC Infect Dis 17(1):151. https://doi.org/10.1186/s12879-017-2246-7
25. Gill AJ, Kovacsics CE, Cross SA, Vance PJ, Kolson LL, Jordan-Sciutto KL, Gelman BB, Kolson DL (2014) Heme oxygenase-1 deficiency accompanies neuropathogenesis of HIV-associated neurocognitive disorders. J Clin Invest 124(10):4459–4472. https://doi.org/10.1172/JCI72279
26. Oka S, Leon J, Sakumi K, Ide T, Kang D, LaFerla FM, Nakabeppu Y (2016) Human mitochondrial transcriptional factor A breaks the mitochondria-mediated vicious cycle in Alzheimer s disease. Sci Rep 6:37889. https://doi.org/10.1038/srep37889
27. Nooka S, Ghorpade A (2018) Organellar stress intersects the astrocyte endoplasmic reticulum, mitochondria and nucleolus in HIV associated neurodegeneration. Cell Death Dis 9(3):317. https://doi.org/10.1038/s41419-018-0341-3
28. Morgello S, Gelman BB, Kozlowski PB, Vinters HV, Masliah E, Cornford M, Cavert W, Marra C et al (2001) The National NeuroAIDS Tissue Consortium: a new paradigm in brain banking with an emphasis on infectious disease. Neuropathol Appl Neurobiol 27(4):326–335
29. Somsouk M, Dunham RM, Cohen M, Albright R, Abdel-Mohsen M, Liegler T, Lifson J, Piatak M et al (2014) The immunologic effects of mesalamine in treated HIV-infected individuals with incomplete CD4+ T cell recovery: a randomized crossover trial. PloS one 9(12):e116306. https://doi.org/10.1371/journal.pone.0116306
30. Thomas JA, Gagliardi TD, Alvord WG, Lubomirski M, Bosche WJ, Gorelick RJ (2006) Human immunodeficiency virus type 1 nucleocapsid zinc-finger mutations cause defects in reverse transcription and integration. Virology 353(1):41–51. https://doi.org/10.1016/j.virol.2006.05.014
31. Geiss GK, Bumgarner RE, Birditt B, Dahl T, Dowidar N, Dunaway DL, Fell HP, Ferree S et al (2008) Direct multiplexed measurement of gene expression with color-coded probe pairs. Nat Biotechnol 26(3):317–325. https://doi.org/10.1038/nbt1385
32. Ritchie ME, Phipson B, Wu D, Hu Y, Law CW, Shi W, Smyth GK (2015) Limma powers differential expression analyses for RNA-sequencing and microarray studies. Nucleic Acids Res 43(7):e47. https://doi.org/10.1093/nar/gkv007
33. Troyanskaya O, Cantor M, Sherlock G, Brown P, Hastie T, Tibshirani R, Botstein D, Altman RB (2001) Missing value estimation methods for DNA microarrays. Bioinformatics 17(6):520–525
34. Scagnolari C, Monteleone K, Selvaggi C, Pierangeli A, D'Ettorre G, Mezzaroma I, Turriziani O, Gentile M et al (2016) ISG15 expression correlates with HIV-1 viral load and with factors regulating T cell response. Immunobiology 221(2):282–290. https://doi.org/10.1016/j.imbio.2015.10.007
35. Schneider WM, Chevillotte MD, Rice CM (2014) Interferon-stimulated genes: a complex web of host defenses. Annu Rev Immunol 32:513–545. https://doi.org/10.1146/annurev-immunol-032713-120231
36. Fagone P, Nunnari G, Lazzara F, Longo A, Cambria D, Distefano G, Palumbo M, Nicoletti F et al (2016) Induction of OAS gene family in HIV monocyte infected patients with high and low viral load. Antiviral Res 131:66–73. https://doi.org/10.1016/j.antiviral.2016.04.009

37. Rosebeck S, Leaman DW (2008) Mitochondrial localization and pro-apoptotic effects of the interferon-inducible protein ISG12a. Apoptosis 13(4):562–572. https://doi.org/10.1007/s10495-008-0190-0
38. Camargo N, Goudriaan A, van Deijk AF, Otte WM, Brouwers JF, Lodder H, Gutmann DH, Nave KA et al (2017) Oligodendroglial myelination requires astrocyte-derived lipids. PLoS Biol 15(5): e1002605. https://doi.org/10.1371/journal.pbio.1002605
39. Voskuhl RR, Itoh N, Tassoni A, Matsukawa MA, Ren E, Tse V, Jang E, Suen TT et al (2019) Gene expression in oligodendrocytes during remyelination reveals cholesterol homeostasis as a therapeutic target in multiple sclerosis. Proc Natl Acad Sci U S A 116(20): 10130–10139. https://doi.org/10.1073/pnas.1821306116
40. Wendelken LA, Jahanshad N, Rosen HJ, Busovaca E, Allen I, Coppola G, Adams C, Rankin KP et al (2016) ApoE epsilon4 is associated with cognition, brain integrity, and atrophy in HIV over age 60. J Acquir Immune Defic Syndr 73(4):426–432. https://doi.org/10.1097/QAI.0000000000001091
41. Shimano H (2002) Sterol regulatory element-binding protein family as global regulators of lipid synthetic genes in energy metabolism. Vitam Horm 65:167–194
42. Siangphoe U, Archer KJ (2015) Gene expression in HIV-associated neurocognitive disorders: a meta-analysis. J Acquir Immune Defic Syndr 70(5):479–488. https://doi.org/10.1097/QAI.0000000000000800
43. Sagar V, Pilakka-Kanthikeel S, Martinez PC, Atluri VSR, Nair M (2017) Common gene-network signature of different neurological disorders and their potential implications to neuroAIDS. PLoS One 12(8):e0181642. https://doi.org/10.1371/journal.pone.0181642
44. Furman D, Chang J, Lartigue L, Bolen CR, Haddad F, Gaudilliere B, Ganio EA, Fragiadakis GK et al (2017) Expression of specific inflammasome gene modules stratifies older individuals into two extreme clinical and immunological states. Nat Med 23(2):174–184. https://doi.org/10.1038/nm.4267
45. Nissen SK, Hojen JF, Andersen KL, Kofod-Olsen E, Berg RK, Paludan SR, Ostergaard L, Jakobsen MR et al (2014) Innate DNA sensing is impaired in HIV patients and IFI16 expression correlates with chronic immune activation. Clin Exp Immunol 177(1):295–309. https://doi.org/10.1111/cei.12317
46. Thompson MR, Sharma S, Atianand M, Jensen SB, Carpenter S, Knipe DM, Fitzgerald KA, Kurt-Jones EA (2014) Interferon gamma-inducible protein (IFI) 16 transcriptionally regulates type i interferons and other interferon-stimulated genes and controls the interferon response to both DNA and RNA viruses. J Biol Chem 289(34):23568–23581. https://doi.org/10.1074/jbc.M114.554147
47. Jonsson KL, Laustsen A, Krapp C, Skipper KA, Thavachelvam K, Hotter D, Egedal JH, Kjolby M et al (2017) IFI16 is required for DNA sensing in human macrophages by promoting production and function of cGAMP. Nat Commun 8:14391. https://doi.org/10.1038/ncomms14391
48. Sanfilippo C, Pinzone MR, Cambria D, Longo A, Palumbo M, Di Marco R, Condorelli F, Nunnari G et al (2018) OAS gene family expression is associated with HIV-related neurocognitive disorders. Molecular neurobiology 55(3):1905–1914. https://doi.org/10.1007/s12035-017-0460-3
49. Cotto B, Natarajaseenivasan K, Langford D (2019) HIV-1 infection alters energy metabolism in the brain: contributions to HIV-associated neurocognitive disorders. Prog Neurobiol 101616. https://doi.org/10.1016/j.pneurobio.2019.101616
50. Codoni V, Blum Y, Civelek M, Proust C, Franzen O, Cardiogenics C, CADGenomics ILC, Bjorkegren JL et al (2016) Preservation analysis of macrophage gene coexpression between human and mouse identifies PARK2 as a genetically controlled master regulator of oxidative phosphorylation in humans. G3 (Bethesda) 6(10): 3361–3371. https://doi.org/10.1534/g3.116.033894
51. Gupta A, Anjomani-Virmouni S, Koundouros N, Dimitriadi M, Choo-Wing R, Valle A, Zheng Y, Chiu YH et al (2017) PARK2 depletion connects energy and oxidative stress to PI3K/Akt activation via PTEN S-nitrosylation. Mol Cell 65(6):999–1013 e1017. https://doi.org/10.1016/j.molcel.2017.02.019
52. Witte ME, Bol JG, Gerritsen WH, van der Valk P, Drukarch B, van Horssen J, Wilhelmus MM (2009) Parkinson s disease-associated parkin colocalizes with Alzheimer s disease and multiple sclerosis brain lesions. Neurobiol Dis 36(3):445–452. https://doi.org/10.1016/j.nbd.2009.08.009
53. Kang I, Chu CT, Kaufman BA (2018) The mitochondrial transcription factor TFAM in neurodegeneration: emerging evidence and mechanisms. FEBS Lett 592(5):793–811. https://doi.org/10.1002/1873-3468.12989
54. Nasoohi S, Ismael S, Ishrat T (2018) Thioredoxin-interacting protein (TXNIP) in cerebrovascular and neurodegenerative diseases: regulation and implication. Mol Neurobiol 55(10):7900–7920. https://doi.org/10.1007/s12035-018-0917-z
55. Bandera A, Masetti M, Fabbiani M, Biasin M, Muscatello A, Squillace N, Clerici M, Gori A et al (2018) The NLRP3 inflammasome is upregulated in HIV-infected antiretroviral therapy-treated individuals with defective immune recovery. Front Immunol 9:214. https://doi.org/10.3389/fimmu.2018.00214
56. Shimano H, Sato R (2017) SREBP-regulated lipid metabolism: convergent physiology - divergent pathophysiology. Nat Rev Endocrinol 13(12):710–730. https://doi.org/10.1038/nrendo.2017.91
57. Pitale PM, Gorbatyuk O, Gorbatyuk M (2017) Neurodegeneration: keeping ATF4 on a tight leash. Front Cell Neurosci 11:410. https://doi.org/10.3389/fncel.2017.00410
58. Kearns AC, Robinson JA, Shekarabi M, Liu F, Qin X, Burdo TH (2018) Caspase-1-associated immune activation in an accelerated SIV-infected rhesus macaque model. J Neurovirol 24(4):420–431. https://doi.org/10.1007/s13365-018-0630-8
59. Dillman AA, Majounie E, Ding J, Gibbs JR, Hernandez D, Arepalli S, Traynor BJ, Singleton AB et al (2017) Transcriptomic profiling of the human brain reveals that altered synaptic gene expression is associated with chronological aging. Sci Rep 7(1):16890–16812. https://doi.org/10.1038/s41598-017-17322-0
60. Darmanis S, Sloan SA, Zhang Y, Enge M, Caneda C, Shuer LM, Hayden Gephart MG, Barres BA et al (2015) A survey of human brain transcriptome diversity at the single cell level. Proc Natl Acad Sci U S A 112(23):7285–7290. https://doi.org/10.1073/pnas.1507125112